Microscopic Calculation of Collective Excitations in ^{4}He Clusters

S. A. Chin and E. Krotscheck

Center for Theoretical Physics and Department of Physics, Texas A&M University, College Station, Texas 77843

(Received 2 March 1990)

We compute the ground-state structure and collective-excitation energies of ^{4}He droplets at zero temperature. The collective excitations are described by a generalized Feynman theory with inputs of exact one- and two-body densities sampled from a second-order diffusion Monte Carlo algorithm. The monopole transition density shows a pronounced shell structure not accountable by simple Jastrow-type variational trial functions.

PACS numbers: 67.40.Db, 05.30.Jp, 36.40.+d

The study of quantum liquid drops is presently an area of active experimental and theoretical research. While one has a reasonably good description of the ground state[1-3] of clusters of ^{4}He, its spectrum of excited states is uncertain. On the other hand, the excitation spectrum of quantum liquid clusters is experimentally more easily accessible than both the ground-state structure and its energetics.[4] An unambiguous determination of finite-size effects in the energy of collective excitations would also help to answer questions relating to the onset of superfluidity as well as resolving the long-standing problem of the relationship between the energy of nuclear giant resonances and the compressibility of nuclear matter.[5]

Recently, estimates of helium-droplet excitation energies have been computed on the basis of a quantized liquid drop,[6] a nonlocal-density-functional theory,[7] and Monte Carlo integrations of analytic, *parametrized* excitation operators.[6,8] Both Refs. 6 and 8 estimate excitation energies on the basis of a variational ground state. By explicitly orthogonalizing these excited states, the authors of Ref. 6 were also able to obtain some higher excitation energies. In Ref. 7, a nonlocal density functional is fitted to reproduce the bulk energetics and surface tension of liquid ^{3}He.

Our approach is distinguished from all previous work by (1) making no assumptions on the density profile (as in Ref. 6) or the energy functional of the clusters (as in Refs. 6 and 7), (2) computing the excitation energies on the basis of the exact ground state (in contrast to Refs. 6 and 8), and (3) determining the *optimal* excitation functions and excitation energies simultaneously by directly solving the generalized Feynman eigenvalue equation, Eq. (7) below. This last distinction is especially important in that *we do not need to redo Monte Carlo integrations to optimize parameters or orthogonalize functions.* The entire excitation spectrum is obtained and wave functions are automatically orthogonal. Our approach is limited only by (a) the statistical and extrapolation errors in sampling the exact one- and two-body ground-state densities and (b) the adequacy of the Feynman ansatz, Eq. (1) below.

We require a translationally invariant solution of the N-particle Schrödinger equation, $\Psi_0(\mathbf{r}_1,\ldots,\mathbf{r}_N)=\Psi_0(\mathbf{r}_1+\mathbf{r},\ldots,\mathbf{r}_N+\mathbf{r})$, for example, as evolved by the Monte Carlo methods described in Ref. 3. Following Feynman,[9] we write a trial function of the excited state as

$$\Psi_F(\mathbf{r}_1,\ldots,\mathbf{r}_N)=F(\mathbf{r}_1,\ldots,\mathbf{r}_N)\Psi_0(\mathbf{r}_1,\ldots,\mathbf{r}_N)\,, \tag{1}$$

where

$$F(\mathbf{r}_1,\ldots,\mathbf{r}_N)=\sum_{i=1}^{N}[f(\mathbf{r}_i-\mathbf{r}_{\text{c.m.}})-\langle f_i\rangle]\,,$$

$$\langle f_i\rangle=\langle\Psi_0|f(\mathbf{r}_i-\mathbf{r}_{\text{c.m.}})|\Psi_0\rangle\,,$$

and $\mathbf{r}_{\text{c.m.}}$ is the center-of-mass coordinate.

Since $\Psi_0(\mathbf{r}_1,\ldots,\mathbf{r}_N)$ is the *exact,* translationally invariant ground-state wave function, the energy difference between the ground state and the trial excited state can be expressed as

$$E_F-E_0=\frac{1}{2}\frac{\langle\Psi_0|[F,[T,F]]|\Psi_0\rangle}{\langle\Psi_0|F^2|\Psi_0\rangle}=\frac{\hbar^2}{2m}\frac{(1-1/N)\int d^3r\,\rho_1(\mathbf{r})|\nabla f(\mathbf{r})|^2-(1/N)\int d^3r\,d^3r'\rho_2(\mathbf{r},\mathbf{r}')\nabla f(\mathbf{r})\cdot\nabla f(\mathbf{r}')}{\int d^3r\,\rho_1(\mathbf{r})|f(\mathbf{r})|^2+\int d^3r\,d^3r' f(\mathbf{r})[\rho_2(\mathbf{r},\mathbf{r}')-\rho_1(\mathbf{r})\rho_1(\mathbf{r}')]f(\mathbf{r}')}\,, \tag{2}$$

where $E_F=\langle\Psi_F|H|\Psi_F\rangle/\langle\Psi_F|\Psi_F\rangle$ is the energy corresponding to the wave function (1), and E_0 is the exact ground-state energy. The coordinates in the second part of Eq. (2) are measured from the center of mass, and the one- and two-body densities are defined by

$$\rho_1(\mathbf{r})=\int d^3r_1\cdots d^3r_N\sum_i\delta(\mathbf{r}_i-\mathbf{r}_{\text{c.m.}}-\mathbf{r})\Psi_0^2,\quad \rho_2(\mathbf{r},\mathbf{r}')=\int d^3r_1\cdots d^3r_N\sum_{i\neq j}\delta(\mathbf{r}_i-\mathbf{r}_{\text{c.m.}}-\mathbf{r})\delta(\mathbf{r}_j-\mathbf{r}_{\text{c.m.}}-\mathbf{r}')\Psi_0^2\,. \tag{3}$$

The energy difference $\hbar\omega\equiv E_F-E_0$ determined by Eq. (2) is an upper bound to the exact excitation energy.

It is convenient to define $u(\mathbf{r})=\sqrt{\rho_1(\mathbf{r})}\,f(\mathbf{r})$ so that Eq. (2) can be written symmetrically as

$$\hbar\omega=\frac{\int d^3r\,d^3r'\,u(\mathbf{r})H_1(\mathbf{r},\mathbf{r}')u(\mathbf{r}')}{\int d^3r\,d^3r'\,u(\mathbf{r})S(\mathbf{r},\mathbf{r}')u(\mathbf{r}')}\,, \tag{4}$$

with the coordinate-space representation of the static structure function

$$S(\mathbf{r},\mathbf{r}')=\delta(\mathbf{r}-\mathbf{r}')+\frac{\rho_2(\mathbf{r},\mathbf{r}')-\rho_1(\mathbf{r})\rho_1(\mathbf{r}')}{[\rho_1(\mathbf{r})\rho_1(\mathbf{r}')]^{1/2}}\,, \tag{5}$$

and the nonlocal kinetic-energy operator

$$H_1(\mathbf{r},\mathbf{r}')=-\left[1-\frac{1}{N}\right]\delta(\mathbf{r}-\mathbf{r}')\frac{\hbar^2}{2m}\frac{1}{[\rho_1(\mathbf{r})]^{1/2}}\nabla\rho_1(\mathbf{r})\cdot\nabla\frac{1}{[\rho_1(\mathbf{r})]^{1/2}}-\frac{\hbar^2}{2mN}\frac{\nabla_{\mathbf{r}}\cdot\nabla'_{\mathbf{r}}\rho_2(\mathbf{r},\mathbf{r}')}{[\rho_1(\mathbf{r})\rho_1(\mathbf{r}')]^{1/2}}\,. \tag{6}$$

The lowest upper bound for the excitation energy is obtained by minimizing the energy difference $\hbar\omega$ with respect to the excitation function $u(\mathbf{r})$. This leads to the desired generalization of the Feynman dispersion relation[9]

$$H_1u(\mathbf{r})=\hbar\omega\int d^3r'\,S(\mathbf{r},\mathbf{r}')u(\mathbf{r}')\,. \tag{7}$$

In contrast to the case of bulk liquid helium, the lack of experimental information on the pair distributions for quantum liquid drops precludes one from using Eq. (7) to predict the spectra of collective excitations from measurements of the structure function. However, since the pair-distribution function can be obtained accurately by an exact solution of the Schrödinger equation, it is a simple matter of solving the eigenvalue problem (7) to obtain the excited states.

The eigenvalue problem (7) can be decoupled and solved by expanding the excitation function and the pair-distribution function in partial waves,

$$u(\mathbf{r})=\sum_l u_l(r)P_l(\hat{\mathbf{r}}\cdot\hat{\mathbf{z}})\,, \tag{8}$$

$$\frac{\rho_2(\mathbf{r},\mathbf{r}')-\rho_1(\mathbf{r})\rho_1(\mathbf{r}')}{[\rho_1(\mathbf{r})\rho_1(\mathbf{r}')]^{1/2}}=\sum_l\frac{2l+1}{4\pi}h_l(r,r')P_l(\hat{\mathbf{r}}\cdot\hat{\mathbf{r}}')\,. \tag{9}$$

Having calculated the excitation function, we obtain finally the transition density,

$$\begin{aligned}\delta\rho_1(\mathbf{r})&=\int d^3r_1\cdots d^3r_N\sum_i\delta(\mathbf{r}_i-\mathbf{r}_{\text{c.m.}}-\mathbf{r})F(\mathbf{r}_1,\ldots,\mathbf{r}_N)\Psi_0^2(\mathbf{r}_1,\ldots,\mathbf{r}_N)\\&=\rho_1(\mathbf{r})f(\mathbf{r})+\int d^3r'[\rho_2(\mathbf{r},\mathbf{r}')-\rho_1(\mathbf{r})\rho_1(\mathbf{r}')]f(\mathbf{r}')\,.\end{aligned} \tag{10}$$

It is worth noting here that both the left- and the right-hand side of Eq. (7) have *two* exact zero-energy eigenfunctions $u_0(\mathbf{r})=\sqrt{\rho_1(\mathbf{r})}$ and $u_1(\mathbf{r})=\mathbf{c}\cdot\mathbf{r}\sqrt{\rho_1(\mathbf{r})}$, where $\mathbf{c}$ is an arbitrary constant vector. Both of these states are spurious: The first, which is a monopole state corresponding to a constant correlation operator, vanishes identically when the ground-state expectation value is subtracted. The second, a dipole state corresponding to a correlation function $f(\mathbf{r})=\mathbf{c}\cdot\mathbf{r}$, again vanishes identically, since in this case $F(\mathbf{r}_1,\ldots,\mathbf{r}_N)=\sum_{i=1}^N f(\mathbf{r}_i-\mathbf{r}_{\text{c.m.}})=0$.

Since one is mainly interested in excitations with low-angular momentum (i.e., monopole and quadrupole excitations), it is only necessary to compute partial-wave amplitudes $h_l(r,r')$ of the pair-distribution function for small values of l. The center-of-mass correction term (last term) in Eq. (6) couples neighboring even and odd multipoles of the two-body density (9). We found, however, that apart from guaranteeing one exact zero-energy eigenvalue in the dipole channel, its effect is very small and can be safely ignored.

Employing the Aziz[10] potential, we evolve the product state $\Psi_0\Phi_0$ of a N-atom helium cluster by a second-order diffusion Monte Carlo (DMC) algorithm DMC2b as developed by one of us in Ref. 3. The variational trial function Φ_0 used is of the McMillian form,

$$\Phi_0=\prod_{i<j}\exp\{-\tfrac{1}{2}(a/r_{ij})^5\}\prod_i\exp\{-\tfrac{1}{2}b^{-2}(\mathbf{r}_i-\mathbf{r}_{\text{c.m.}})^2\}\,, \tag{11}$$

which is manifestly translationally invariant. The ground-state properties thus obtained for helium clusters

TABLE I. $\varepsilon_0=E_0/N$ is the ground-state energy per particle in units of K, $r_0=(\frac{5}{3})^{1/2}\langle r^2\rangle^{1/2}N^{-1/3}$ is the unit radius defined from $\mathbf{r}_{\text{c.m.}}$ in units of Å, the $\hbar\omega$ are the collective-excitation energies in units of K (numbers inside brackets are the corresponding VMC results), and Δt^* is the reduced time-step size in units of Å$^{-1/2}$ such that $\langle\Delta r^2\rangle=\Delta t^*$. VMC results are obtained by using trial function (11); GFMC results are taken from Ref. 1. All DMC results are obtained by using algorithm DMC2b of Ref. 3, except for the case 3.9†, which uses algorithm DMC2a as a check.

N	Δt^*	b	$\varepsilon_0^{\text{VMC}}$	$\varepsilon_0^{\text{DMC}}$	$\varepsilon_0^{\text{GFMC}}$	r_0^{VMC}	r_0^{DMC}	r_0^{GFMC}	$\hbar\omega(l=0)$	$\hbar\omega(l=2)$
40	0.002	3.6	−2.196(1)	−2.525(3)	−2.487(3)	2.630(1)	2.551(2)	2.57	3.60[3.44]	1.37[1.77]
	0.002	3.5	−2.194(1)	−2.529(3)		2.595(1)	2.532(2)		3.53[3.58]	1.50[1.84]
70	0.001	3.9	−2.744(1)	−3.188(2)	−3.12(4)	2.536(1)	2.441(2)	2.47	3.94[3.38]	1.50[1.52]
	0.001	3.9†		−3.176(3)			2.475(3)		3.91	1.44
	0.0005	3.8	−2.736(2)	−3.170(2)		2.505(1)	2.461(3)		3.96[3.53]	1.54[1.60]
112	0.0005	4.3	−3.143(2)	−3.702(3)	−3.60(1)	2.491(1)	2.399(2)	2.44	3.92[2.97]	1.76[1.27]
	0.0005	4.2	−3.134(1)	−3.705(3)		2.465(1)	2.391(2)		4.27[3.16]	1.62[1.34]

of size $N=40$, 70, and 112 are tabulated in Table I and compared with the Green's-function Monte Carlo (GFMC) result of Ref. 1. For the present calculation, much better statistics is required than for the calculation of the ground-state energy, since one not only needs to bin the one-body density, but also the two-dimensional partial-wave amplitudes $h_l(r,r')$. Typically, after equilibrating 2000 four-hit Metropolis sweeps, $(2\text{-}5)\times10^5$ configurations are sampled for the variational calculation. For the DMC calculation, a target population of 200 configurations is maintained. After equilibrating for 2000 time steps, the evolution is continued for 40000–60000 time steps. The statistical errors for the ground-state energy given in Table I are from block averages of 50 time steps.

We have checked that the trial and the normalization (growth) estimate of the ground-state energy are independent of the trial function used and agree with each other to three significant digits. We have also checked the time-step convergence error by doubling the time-step size and by running an entirely different second-order algorithm, algorithm DMC2a of Ref. 3. Systematic changes on the order of 1% are observed. Although these are sometimes larger than the quoted statistical errors, they are not significant for our purpose. More serious is the extrapolation error incurred by using the perturbative estimate

$$\langle\Psi_0|O|\Psi_0\rangle=2\langle\Psi_0|O|\Phi_0\rangle-\langle\Phi_0|O|\Phi_0\rangle \tag{12}$$

for computing the ground-state expectation value of operators other than the Hamiltonian. To gauge this error, we check that consistent values for $\langle r^2\rangle$ are obtained for each cluster size according to Eq. (12) from independent runs with slightly different values of b. The parameter a is fixed at $a=3.0$. Table I shows that the unit radius $r_0=(\frac{5}{3})^{1/2}\langle r^2\rangle^{1/2}N^{-1/3}$ thus obtained is independent of b to within 1% or less. Our cluster radii and energies are both systematically below previous GFMC results.

Figures 1(a)–1(c) give the one-body densities as obtained by applying Eq. (12) bin by bin to 60 bins. The bin sizes used were 0.3 Å for $N=40$, 70, and 0.32 Å for $N=112$. For short runs, we observed large oscillations in the density similar to those noted in Ref. 1. In our production runs, which iterate an order of magnitude more generations than those of Ref. 1, these fluctuations have largely disappeared. However, small oscillations persist and the density in the first few bins remains affected by relatively large statistical errors. The partial-wave amplitudes $h_l(r,r')$ for $l=0$, 1, and 2 are obtained by a $30\times59=1770$ binning of the two-body density with the same bin size as in the one-body-density case. The statistical fluctuations at $r\approx r'\approx0$ remain large; fortunately, they carry little weight in determining the excited-state energies.

The inputs to Eq. (10) are the one- and two-body densities that were calculated as described above. In solving for the excited states, a modest smoothing of the one-body density around the origin was necessary for the calculation of the second derivative appearing in the kinetic-energy operator H_1 of Eq. (7). In the outer surface, where the density falls below 2% of the central density, and statistics is very poor, we extrapolated the density by its asymptotic form $\rho_1(\mathbf{r})\sim\exp[-2(2m\mu/$

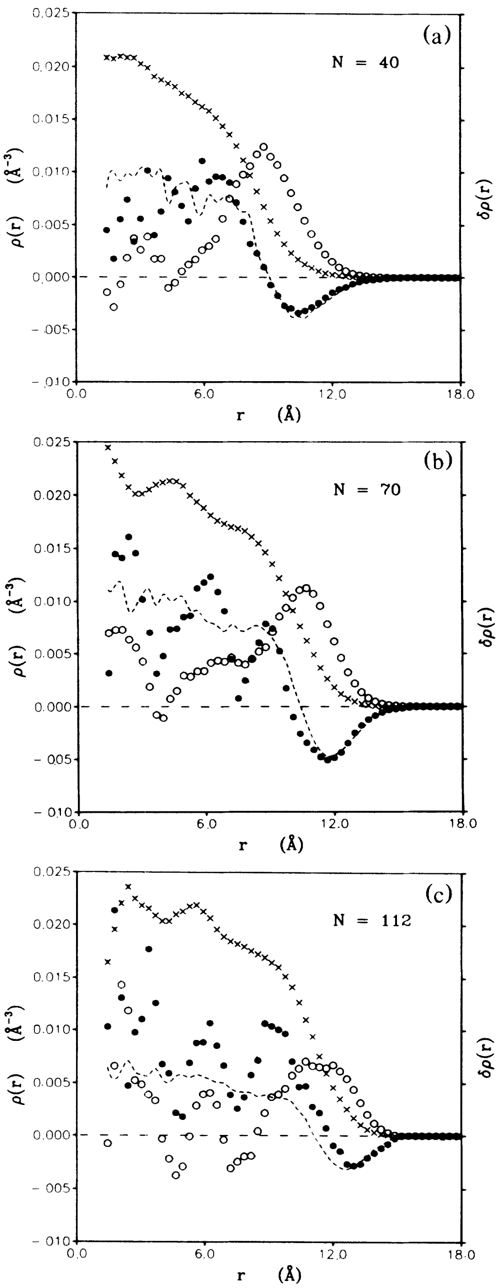

FIG. 1. (a) The one-body density (crosses) and transition densities for the monopole (solid circles) and the quadrupole (open circles) collective mode of a $N=40$ helium cluster. The dotted line is the monopole transition density as calculated from the variational wave function (11). (b) Same as (a) for a $N=70$ helium cluster. (c) Same as (a) for a $N=112$ helium cluster.

$\hbar^2)^{1/2}r]/r^2$. The localized excitations are discrete solutions of Eq. (7) corresponding to bound states; i.e., those with energies $\hbar\omega$ satisfy $\hbar\omega+\mu<0$. Since our ground-state energies are in general agreement with those of Ref. 1, we consider it adequate to use their fitted mass formula to compute the chemical potential $\mu \equiv dE/dN = -7.02+12.53x-3.73x^2$, where $x=N^{-1/3}$. For $N=40$, 70, and 112, the chemical potential is, respectively, $\mu=-3.67$, -4.12, and -4.58 K.

Our results for the monopole and quadrupole excitation energies for droplet sizes $N=40$, 70, and 112 are also given in Table I. The variational Monte Carlo (VMC) results are obtained by solving the eigenvalue equation (7) with inputs of one- and two-body densities sampled from the trial function (11). Despite very different ground-state variational functions and a completely different method of optimizing the excitation function, our VMC quadrupole energies are surprisingly close to those obtained in Ref. 8. (For $N=40$, 70, and 112, their monopole and quadrupole energies are 2.79,2.75,2.63 and 1.72,1.46,1.28 K, respectively.) Both our VMC and DMC excitation energies are significantly different from the liquid-drop-model (LDM) prediction of $\hbar\omega(l=0)=25.6N^{-1/3}$ K ($=7.49$, 6.21, and 5.31 K) and $\hbar\omega(l=2)=10.4N^{-1/2}$ K ($=1.64$, 1.24, and 0.98 K). Our DMC results do not even begin to share the same trend as LDM predictions. We conclude therefore that, for the cluster sizes considered, the detail dynamics of helium clusters is far from the liquid-drop limit. By comparing results from independent ground-state runs with different variational parameters, we estimate that our excitation energies have systematic extrapolation errors on the order of 10%.

Figures 1(a)-1(c) also show the transition densities $\delta\rho_l(\mathbf{r})$ [cf. Eq. (10)] for the monopole and the quadrupole excitations for $N=40$, 70, 112. In all three cases, the quadrupole excitation has the expected form of a surface mode. Our results for the monopole excitation are of particular interest: While the ground-state density is reasonably smooth, the monopole transition density shows remarkable oscillations for $N=70$ and 112. (In the $N=40$ case, the monopole excitation energy is very close to the continuum and we were unable to distinguish systematic oscillation from numerical fluctuations.) We believe that these oscillations are significant since they are a stable feature of all our larger-cluster calculations and have an average wavelength (3.4 Å for $N=70$ and 2.8 Å for $N=112$) of approximately the average particle separation. We found such oscillations in our calculations independent of the time-step size and the choice of the algorithm. Moreover, they are visible even in the directly sampled partial-wave amplitude $h_l(r,r')$. The oscillations of the transition density are evidently connected with the geometric, hard-sphere-like, shell structure of the droplets. Figures 1(a)-1(c) also show the monopole transition density obtained from the variational Monte Carlo calculation with a simple McMillan-type Jastrow wave function (11). None of the shell structure is observed in this case.

We have presented and applied in this paper a generalized Feynman theory for computing collective excitations of a finite system from knowledge of the ground-state one- and two-body densities. Our approach depends on the availability of a high-statistics ground-state density distribution made possible by present-day supercomputers. In computing for the excited states, we have also found a somewhat unexpected shell structure of the transition density for the monopole resonance which is evidently related to the hard-core-like interaction of ^{4}He atoms.

This work was supported, in part, by the National Science Foundation Grants No. PHY89-07986 (to S.A.C.) and No. PHY-8806265 (to E.K.), the Robert A. Welch Foundation Grant No. A-1111, and the Texas Advanced Research Program under Grant No. 010366-012 (to E.K.). Discussions with S. Shlomo and S. Stringari are gratefully acknowledged. The calculations were performed on the CRAY-YMP computer of the Texas A&M University Supercomputer Center.

---

[1] V. R. Pandharipande, J. G. Zabolitzky, S. C. Pieper, R. B. Wiringa, and U. Helmbrecht, Phys. Rev. Lett. **50**, 1676 (1983).

[2] P. Sindzingre, M. J. Klein, and D. M. Ceperley, Phys. Rev. Lett. **63**, 1601 (1989).

[3] S. A. Chin, Texas A&M University, Center for Theoretical Physics, Report No. 66/89, 1989 (unpublished).

[4] S. Gspann, in *Physics of Electronic and Atomic Collisions,* edited by S. Datz (North-Holland, Amsterdam, 1982), p. 79ff.

[5] A. Bohr and B. Mottelson, *Nuclear Structure* (Benjamin, New York, 1975), Vol. II.

[6] M. V. Rama Krishna and K. B. Whaley, Phys. Rev. Lett. **64**, 1126 (1990); J. Chem. Phys. **93**, 746 (1990).

[7] M. Casas and S. Stringari, J. Low Temp. Phys. **79**, 135 (1990).

[8] R. B. Wiringa, S. C. Pieper, and V. R. Pandharipande, Argonne National Laboratory Report No. Phy-4676-TH-85, 1985 (to be published).

[9] R. P. Feynman, Phys. Rev. **94**, 262 (1954).

[10] R. A. Aziz, V. P. S. Nain, J. C. Carley, W. L. Taylor, and G. T. McConville, J. Chem. Phys. **70**, 4330 (1979).